Molecular Immunology 106 (2019) 119–126

Contents lists available at ScienceDirect

Molecular Immunology

journal homepage: www.elsevier.com/locate/molimm

TIMP-3 suppression induces choroidal neovascularization by moderating the polarization of macrophages in age-related macular degeneration

Ying Cheng, Tongjie Cheng, Yi Qu*

Department of Geriatrics, Qilu Hospital of Shandong University, No. 107, Wenhuaxi Road, Jinan, 250012, China

ARTICLE INFO

Keywords:
Choroidal neovascularization
Macrophages
Polarization
Tissue inhibitor of metalloproteinases–3

ABSTRACT

Purpose: To investigate the role of tissue inhibitor of metalloproteinases–3 (TIMP-3) as a key moderator of macrophage polarization in choroidal neovascularization (CNV) lesions of model mice and in bone marrow-derived macrophage (BMDM).

Method: We used siR-TIMP-3 to transfect BMDM and gave an intravitreal injection of siR-TIMP-3 to laser-induced CNV mice model, real time-PCR and western blot were applied for detecting the expressions of TIMP-3 and macrophages' biomarker. Besides, CNV lesions in different treatment groups of animal model were examined by the optical coherence tomography angiography (OCTA).

Results: Our experimental data showed that lack of TIMP-3 stimulated M2 polarization proved by real time-PCR and western blot in BMDMs and CNV mice model. Moreover, intravitreal injection of siR-TIMP-3 accelerated CNV formation using OCTA, which indicated that TIMP-3 suppression is related to pro-angiogenesis of M2 macrophage.

Conclusion: We showed that the absence of TIMP-3 leads to a more pro-angiogenic microenvironment, playing a key role in CNV formation by positively modulating M2 polarization. The role of TIMP-3 in the regulating inflammation and novel therapeutic target of nAMD needs to be further studied.

1. Introduction

Choroidal neovascularization (CNV) arises from choriocapillaris and grows into subretinal space and retina, which is the major pathological feature associated with neovascular age-related macular degeneration (nAMD), potentially leading to serious complications including fluid accumulation and subretinal hemorrhage with visual impairment outcomes (Lim et al., 2012).

Currently, intravitreal anti-vascular endothelial growth factor (VEGF) become the first-line therapy for nAMD, which can regulate the function of VEGF effectively and play a role in preventing abnormal angiogenesis and lessening exudation (Jager et al., 2008). However, the mechanisms upstream of VEGF secretion remain largely unclear. Recent advances have highlighted that the process of nAMD is accompanied by the recruitment of inflammatory cells to neovascularization lesion, the consequence of which is the expression of numerous cytokines and chemokines that induce angiogenesis.

Macrophages have long been localized to sites of CNV in patients with human AMD (Penfold et al., 2001). So far, the role of macrophage polarization in nAMD development has not been well characterized. Espinosa-Heidmann et al. (Espinosa-Heidmann et al., 2003) showed that experimental depletion of macrophages decreases choroidal neovascularization in laser-injured mice, while others held a contrary point with macrophages inhibiting CNV development (Apte et al., 2006). The contradictory findings of macrophages that have been observed in CNV lesion might be explained by differential macrophage polarization with respect to M1 macrophages and M2 macrophages. The M1 macrophages (inducible nitric-oxide synthase, iNOS+), which could be triggered by bacterial lipopolysaccharides or interferon-γ, have been proved to inhibit angiogenesis. Besides, the M2 macrophages (Arginase-1, Arg1+), which develop in response to IL-4, IL-10 or PGE2 stimulation, are considered to promote pathological angiogenesis (Gordon and Martinez, 2010; Sica et al., 2015). Although the key cytokine regulators of macrophage polarity have been identified, the functional heterogeneity of these effector leukocytes can be further honed by both tissue environmental factors and other cell autonomous mediators.

Tissue inhibitor of metalloproteinases–3 (TIMP-3) belongs to a family of genes encoding for inhibitors of matrix metalloproteinases, a group of zinc-binding endopeptidases involved in the degradation of the extracellular matrix. TIMP3 has been shown by other studies to play an important functional role in inflammation (Casagrande et al., 2012; Smookler et al., 2006). Smookler et al. demonstrated that TIMP-3

* Corresponding author.
E-mail address: yiqucn@sdu.edu.cn (Y. Qu).

https://doi.org/10.1016/j.molimm.2018.12.026
Received 28 October 2018; Received in revised form 17 December 2018; Accepted 24 December 2018
Available online 27 December 2018

regulates the shedding of TNF-a or its receptor from the cell surface of macrophages and Sean E. Gill and his colleagues showed that TIMP-3 leads to alter the macrophage function in lung injury (Gill et al., 2013; Smookler et al., 2006). However, whether TIMP-3 is involved in CNV development in nAMD eyes by targeting macrophage polarization is still unknown. In this study, we confirm the role of TIMP-3 in regulating inflammation and CNV lesions of nAMD animal model.

2. Materials and methods

2.1. Animals and ethics statement

The present study conformed to the Guide for the Care and Use of Laboratory Animals of the United States National Institutes of Health and the ARVO Statement for the Use of Animals in Ophthalmic and Vision Research. The protocols were approved by the Shandong University Qilu hospital. C57BL/6 J mice used in this study were provided by the animal facility of Shandong University and Brown Norway (BN) rats were purchased from Vitalriver (Beijing, China).

2.2. Cell culture and transfection

Bone marrow-derived macrophages (BMDM) was isolated from C57BL/6 J mice cultured for 7 days, as described elsewhere (Gill et al., 2010; Tanino et al., 2010). Specifically, the femur and tibia of both hind legs were isolated and freed of all soft tissue following euthanasia. Femurs and tibias were removed from mice and crushed in a sterile mortar in presence of 1% FBS/PBS, and filtered. Cells were washed, resuspended, and cultured in differentiation medium macrophage medium (RPMI 1640, 10% fetal bovine serum and 20 ng/ml macrophage colony-stimulating factor (M-CSF; Peprotech, Rocky Hill, USA)) for 7 days.

SiR-TIMP-3 and scrambled siRNA was purchased from GenePharma (Shanghai, China). Briefly, 30 nM of siR-TIMP-3 were transfected into BMDM (2×10^6 cells/well) using EndoFectin™ Max transfection agent (GeneCopoeia, San Diego, CA, USA). Cells transfected with scrambled siRNA were used as negative control. Total cellular protein and RNA was collected 48 h after transfection.

2.3. Laser-induced CNV model and animal treatment

The laser-induced CNV model was established as described (Apte et al., 2004; Zhao et al., 2013). Briefly, C57BL/6 J mice were anesthetized with ketamine hydrochloride (100 mg/kg body weight) followed by 1% tropicamide (Santen, Osaka, Japan) for pupillary dilation. The four laser spots were created by 532-nm laser (Visulas 532S; Carl Zeiss Meditec, Dublin, Ireland) in a standard fashion around the optic nerve using a slip lamp delivery system and coverslips positioned on the rat cornea as contact lens. Lesions were induced using a power of 200 mW, a spot size of 70 μm, and a duration of 100 ms. Only the laser spots in which a bubble was produced without hemorrhage, indicating perforated Bruch's membranes, were considered effective and included in the study. The rupture of Bruch's membrane was confirmed by the formation of a vaporization bubble. Initially, laser spots were located between vessels in all directions, maintaining the same distance to the optic nerve head.

Eighteen mice were randomly divided into three groups (six animals per group). SiR-TIMP-3 (5 μl of 100 nM) and miRNA negative control (using the same volume as siR-TIMP-3) were packaged EndoFectin Reagent and injected intravitreally. The vehicle group were injected with the same volume of saline and EndoFectin Reagent. Vehicle and drugs were administered intravitreally immediately after laser photocoagulation on day 0, one more injection was performed on day 4 after laser photocoagulation. SiR-TIMP-3 and negative control sequences were designed as below:

Forward-5′ CCAAACACUACGCCUGCAUTT
Reverse-5′ AUGCAGGCGUAGUGUUUGGTT
Forward-5′UUCUUCGAACGUGUCACGUUT (negative control)
Reverse-5′ ACGUGACACGUUCGGAGAATT (negative control)

2.4. Optical coherence tomography angiography images

Fifteen BN rats were randomly divided into three groups (five animals per group), including siR-TIMP-3 (15 μl of 100 nM), negative control and vehicle group. They were performed retinal laser photocoagulation and reagent injection as mentioned above, examined by color fundus photography and optical coherence tomography angiography images (OCTA).

OCTA was performed using the RTVue XR Avanti with AngioVue (Optovue Inc, Fremont, California, USA). The novel technology has been described previously in detail in a number of publications (Ishibazawa et al. 2015; Jia et al., 2012; Quaranta-El Maftouhi et al., 2015). A small platform was built for the stable positioning of the rat in front of the AngioVue device. Images were taken in the deep phase of the general anesthesia after pupil dilatation. $6 \times 6\,mm^2$ scanning dimension has been chosen, the scanning area can be centered on the region of optic nerve including four laser spots.

Using the newly software (AngioAnalytics, Optovue Inc, Fremont, California, USA), it is also possible to contour the CNV in the OCTA and calculate the CNV area based on a binary image of the contoured area. The CNV area is here defined as the total area with active blood flow within the CNV network. The presence of CNV and the CNV area were determined by two retina specialists (Y.C. and TJ.C).

2.5. Western blot analysis

Protein was extracted from BMDMs or RPE/choroidal tissues with RIPA lysis buffer (Solarbio, Beijing, China). The tissue lysates were centrifuged at 12,000 rpm for 10 min at 4 °C, and the supernatants were separated for further analysis. Protein samples (20 μg protein/lane) were separated using 10% SDS-PAGE and then transferred onto PVDF membranes (Merck Millipore, Billerica, MA, USA). The membrane was blocked in Tris-buffered saline containing 5% nonfat milk and 0.1% Tween 20 for 2 h at room temperature and then incubated overnight with primary antibodies: TIMP-3 (ab39184, 1:1000, Abcam, Cambridge, MA, USA), CD80 (AF740, 1 μg/ML; R&D Systems, Minneapolis, MN, USA), iNOS (#13120, 1:1000; CST, Beverly, MA, USA), CD163 (ab182422, 1:1000, Abcam), Arginase-1 (#93668, 1:1000; CST), GAPDH (1:1000; Hangzhou Goodhere Biotechnology Co., Ltd China). After the membranes were washed with PBS, horseradish peroxidase (HRP)-conjugated goat anti-rabbit or anti-mouse secondary antibodies were applied for 1 h at room temperature. After rinsing, the proteins were detected by enhanced chemiluminescence (Merck Millipore). The protein levels were quantified by densitometry and normalized to the corresponding GAPDH level.

2.6. Real-Time PCR

The total RNA from BMDM or RPE/choroidal tissues were extracted using TRIzol reagent (Invitrogen, Carlsbad, CA, USA). RNA then underwent reverse transcription using the Prime Script RT Master Mix kit (TaKaRa, Shiga, Japan) followed by analysis using real-time PCR (RT-PCR) with the SYBR Green PCR Master Mix (TaKaRa) based on the expression of β-actin on Roche LightCycler 480 system. The primers applied for RT-PCR reaction are shown in Table 1.

2.7. Statistical analysis

All data was expressed as means ± SEM. Assessment of statistical significance was done using statistical analysis software SPSS (IBM SPSS Statistics 21; SPSS Inc., Chicago, IL, USA) and GraphPad Prism version 5.0 (GraphPad Software, La Jolla, CA, USA). For comparisons

Table 1
Detailed information of primers.

Primers	Primer sequences (5'-3')	Annealing temperature (∘C)	Product size (bp)
TIMP3	F- GCCTTCTGCAACTCCGACAT R- TCTCGGAAGCTTCCGTATGG	60	166
CD80	F- ACGACTCGCAACCACACCATTAAG R-TGATGACAACGATGACGACGACTG	63	172
TNF-α	F- GCGACGTGGAACTGGCAGAAG R- GCCACAAGCAGGAATGAGAAGAGG	64	103
iNOS	F-TGGTCCGCTAGAGAGTGCT R-CCTCATTGGCCAGCTGCTT;	60	108
CD206	F- ACCTGGCAAGTATCCACAGCATTG R- TGTTGTTCTCATGGCTTGGCTCTC	63	186
Arg-1	F-GCAGAGGTCCAGAAGAATGG, R-AGCATCCACCCAAATGACAC	58	123
Ym-1	F-TCACAGGTCTGGCAATTCTTCTG, R-TGCATTCCAGCAAAGGCATA	59	166
β-actin	F- TTGCCGACAGGATGCAGAA R- GCCGATCCACACGGAGTACT	60	101

between experimental groups, student-t test and one-way analysis of variance (ANOVA) were used as indicated in figure legends. All the P values were two-sided and the differences were considered statistically significant at $P < 0.05$.

3. Results

3.1. The expression of TIMP-3 is downregulated by siRNA in BMDMs

For purpose of evaluating the status of macrophage polarization driven by TIMP-3 in BMDM, we used siR-TIMP-3 and scrambled siRNA to transfected the BMDMs with EndoFectin™ Max transfection agent. Then the RNA and protein were extracted after 48 h of transfection, the RT-PCR and western blotting results of TIMP-3 expression were shown in Fig. 1. The results demonstrated that siR-TIMP3 significantly downregulated the expression level of TIMP-3 in BMDM using RT-PCR ($P = 0.0014$) and western blotting ($P = 0.0048$).

3.2. Macrophage polarization is altered via TIMP-3 regulation in BMDMs

In order to test whether TIMP-3 modulates M1/M2 macrophage polarization, BMDM were transfected with siR-TIMP-3 and siR-NC. After 48 h of transfection, the RNA and protein of BMDM were collected. Fig. 2A represents the mRNA relative expressions of CD80, TNF-α, iNOS, CD206, Arg-1 and Ym-1 in BMDMs. Expression level of CD206, Arg-1 and YM-1 were significantly increased after transfection in siR-TIMP-3 group, accompanied with the decreasing TNF-α expression. Representative blots and the relative gray values were shown in Fig. 2B-C, the expression of iNOS protein in siR-TIMP-3 group statistically decreased, however, the CD163 and Arg-1 protein expression levels were significantly elevated in siR-TIMP-3 group. The trend was consistent with the finding in RT-PCR assay. These results indicated the polarized trend of BMDM that the expressions of M2 macrophage biomarkers increased after the siR-TIMP-3 transfection.

3.3. The expression of TIMP-3 is downregulated by siRNA in laser-induced CNV mice

Eighteen mice were randomly divided into three groups (six animals per group) of siR-TIMP-3, miRNA negative control and vehicle group, they were performed intravitreal injection with three different regents after laser photocoagulation on day 0 and 4. To determine whether TIMP-3 has been suppressed successfully in RPE/choroidal tissues of laser-induced CNV mice, we tested the TIMP-3 mRNA expression level at different time points in three groups. As shown in Fig. 3, the TIMP-3 mRNA expression was significantly decreased at days 1, 3 and 7 after laser photocoagulation in siR-TIMP-3 group comparing with other two groups.

3.4. TIMP-3 regulates macrophage polarization in RPE/Choroidal tissues with laser-induced CNV

To figure out the changes of macrophage polarization effected by siR-TIMP-3 in laser-induced CNV mice eyes, we tested the mRNA relative expression of specific markers of macrophage. The results showed that mRNA expression of CD206, Arg1 and Ym1 significantly upregulated in siR-TIMP-3 group at days 1 and 3 as compared to control, among which CD206 and Arg-1 expression returned to baseline at day 7 after laser photocoagulation in the RPE/choroidal tissues except Ym1, it was still shown a relatively high expression at day 7. In addition, TNF-α mRNA relative expression increased significantly in day 1 after siR-TIMP-3 injection (Fig. 4). Besides, CD80 and iNOS did not show significant differences in three groups at different days.

Representative blots and the relative gray values of CD80, iNOS, CD163 and Arg-1 protein were represented in Fig. 5. The protein expression level of CD80 was detected to be declined substantially at day 3 but increased at day 7, iNOS decreased at day 1 in siR-TIMP-3 group. The CD163 and Arg-1 protein expression showed a significantly increasing trend at days 1 and 3, additionally, Arg-1 still kept a relatively high protein level in day 7 as compared to control. The trend of western blot was consistent with the finding in RT-PCR, which indicated that lack of TIMP-3 will lead to macrophage polarization toward M2 phenotypes with a potential pro-angiogenic capacity in retina.

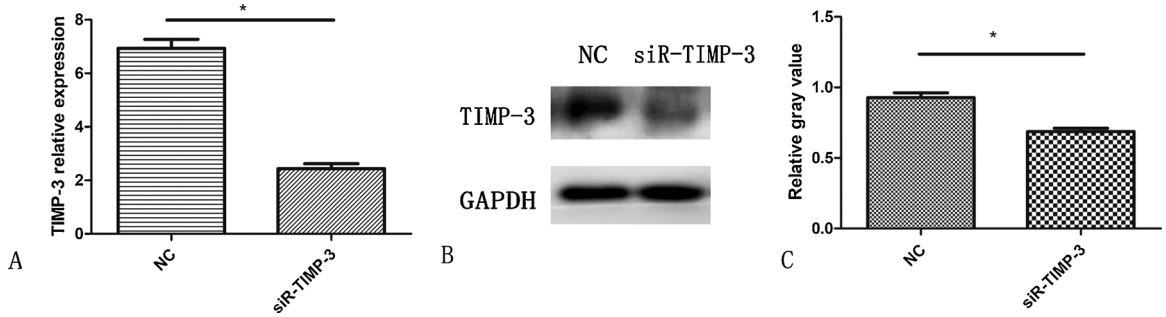

Fig. 1. Expression of TIMP-3 in BMDMs after siRNA transfection. 30 nM of siR-TIMP-3 and scrambled siRNA (negative control) were transfected into BMDM (2×10^6 cells/well) using EndoFectin™ Max transfection agent, respectively. RNA of BMDM in two groups were extracted using TRIzol reagent after 48 h of transfection and then analyzed by RT-PCR. The results showed that the mRNA expression of TIMP-3 was significantly downregulated by siR-TIMP-3 in BMDMs ($P = 0.0014$). The protein expression of TIMP-3 was detected by western blotting and showed decrease in siR-TIMP-3 group ($P = 0.0048$). mRNA expression was relative to β-actin. The protein expressions were relative to GAPDH. Student-t test was used to analyzed the data. *$P < 0.05$, **$P < 0.001$.

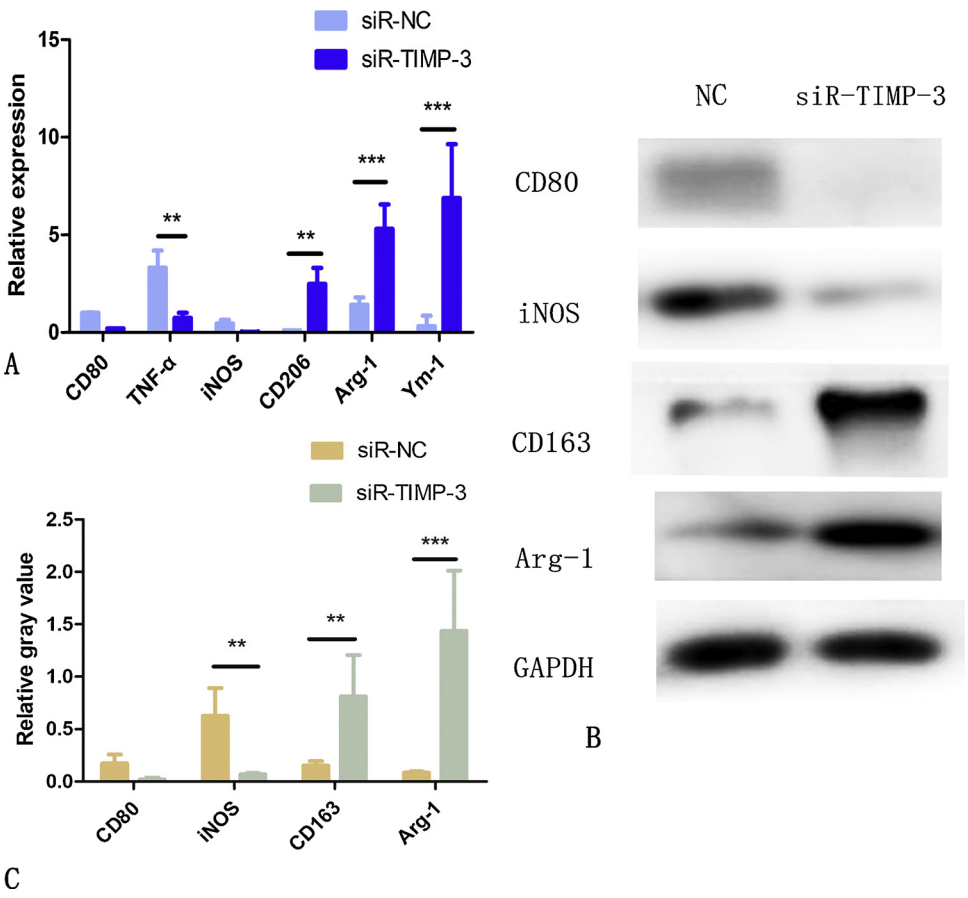

Fig. 2. Expression of CD80, TNF-α, iNOS, CD206, Arg-1 and Ym-1 in BMDMs after siRNA transfection. After 48 h of siR-TIMP-3 (30 nM) and scrambled siRNA (negative control) transfection in BMDMs, mRNA expressions of CD206, Arg-1 and YM-1 were significantly increased in the siR-TIMP-3 group, while that of TNF-α were decreased. CD80 and iNOS mRNA expression were not significantly changed (A). The protein expression of CD163 and Arg-1 were significantly increased in the siR-TIMP-3 group shown by representative blots and relative gray values, accompanying with the iNOS declined (B, C). The gene expressions were detected by RT-PCR and relative to β-actin, the protein expressions were detected by western blotting and relative to GAPDH. Student-t test was used to processed the data. *P < 0.05, **P < 0.001.

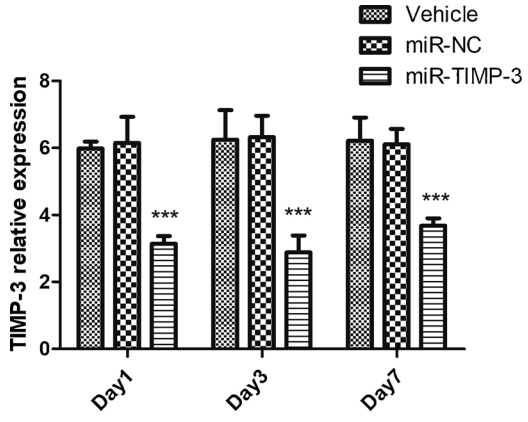

Fig. 3. Gene expression of TIMP-3 in RPE/choroidal tissue of laser-induced CNV mice after siRNA intravitreally injected at different time points. The mRNA level of TIMP-3 significantly decreased at days 1, 3, and 7 in siR-TIMP-3 group. mRNA expression was relative to β-actin. one-way analysis of variance (ANOVA) was used to process the data. Data are presented as mean + SEM, n = 6 for each time point. *P < 0.05, **P < 0.001.

3.5. OCTA images in the laser-induced CNV eyes

Previous studies have reported that inhibition of M2 macrophages can suppress CNV development (Gordon and Martinez, 2010; Sica et al., 2015). Therefore, we planned to make clear whether TIMP-3 suppression could impact on CNV formation and development via targeting M2 polarization. To this end, OCTA was applied for visualizing blood flow of CNV lesion in rats' eyes.

For optimized imaging, the focus in RTVue XR Avanti had to be adjusted manually. The best quality was achieved when the cornea was lubricated during the deep phase of general anesthesia. As OCT angiography imaging takes less than 30 s, anesthetic cataract does not present a big problem OCT angiography in the model of laser-induced CNV. After the OCTA examination, fundus colorized photography was also performed as complemental observation. The OCTA images of retinal perfusion in different retinal layers (superficial, deep, outer retina and the choriocapillaris layers) were represented in Fig. 6A, four laser spots were shown at approximately 3, 6, 9 and 12 o'clock around the optic nerve.

In laser-treated eyes, we acquired the retinal circulation of four different layers as mentioned. The abnormal neovascular vessels were most probably detected in the outer retina and choriocapillaris because of the automatic structure (Fig. 6B). Compared with FFA and OCT, some parameters of CNV lesion can be automatically measured by AngioAnalytics software, which could provide us more helpful quantitative information (Fig. 6C).

3.6. TIMP-3 suppression induced CNV formation after laser-induced photocoagulation

In order to prove whether elevation of M2 macrophages by TIMP-3 inhibition could promote CNV development, we injected miR-TIMP-3 intravitreally immediately after laser photocoagulation and on day 4 to observe the formation of CNV lesion at day 7 by OCTA. Impact of TIMP-3 on CNV structure and flow area was detected by color fundus photography and OCTA, CNV area in each eye was captured and automatically calculated by AngioAnalytics software (Fig. 7). In our study, the mean CNV flow areas of vehicle, miR-NC and miR-TIMP-3 groups are 0.067 ± 0.038, 0.063 ± 0.013 and 0.136 ± 0.041 (P = 0.013), respectively, which demonstrated that intravitreal delivery of miR-TIMP-3 resulted in a significantly larger CNV flow area in comparison to control group at day 7.

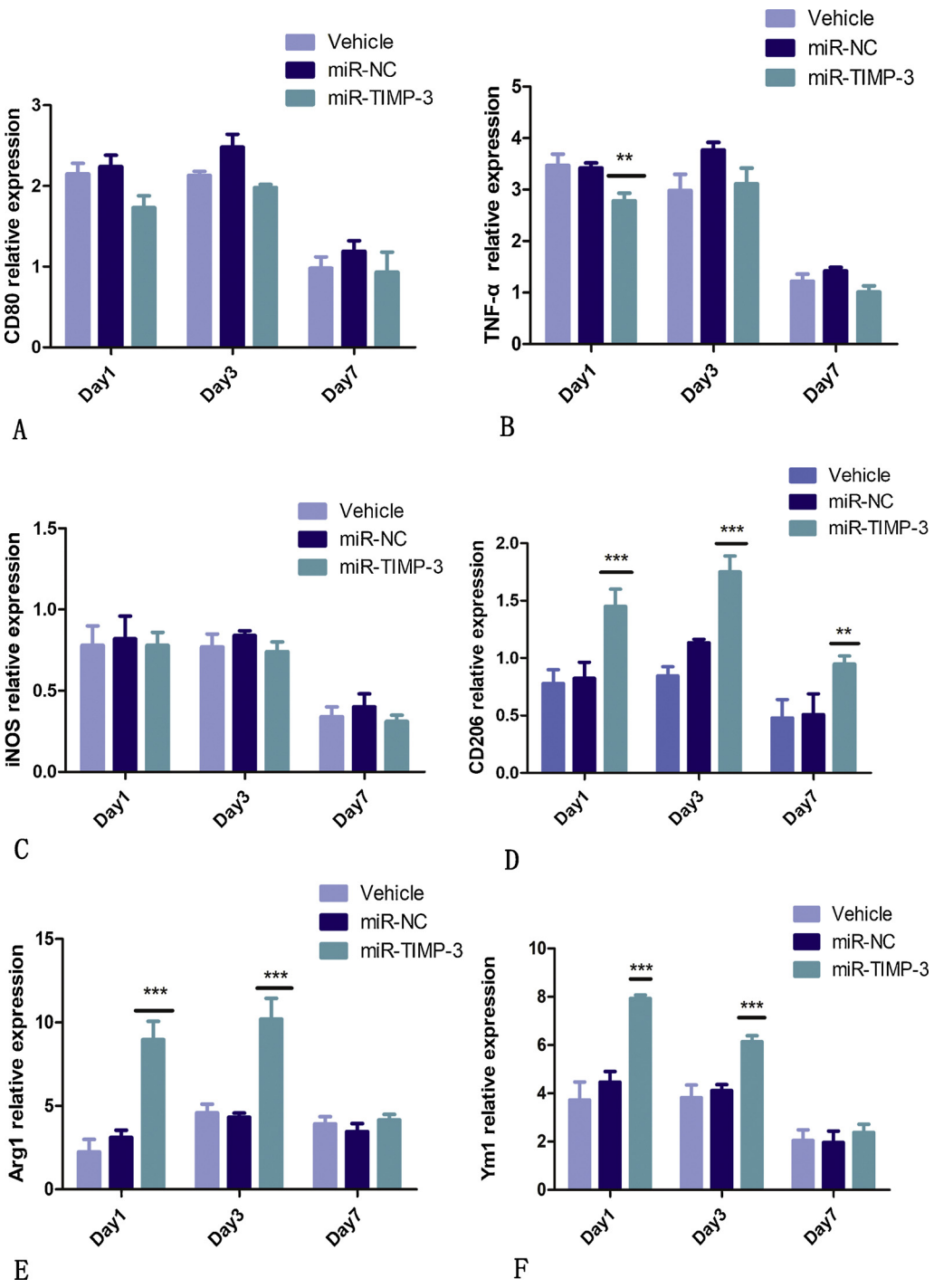

Fig. 4. The mRNA expression level of CD80, TNF-α, iNOS, CD206, Arg-1 and Ym-1 in RPE/choroidal tissue after siRNA-TIMP-3 or negative control intravitreally injected at different time of laser-induced CNV mice. The gene level of TNF-α was elevated at day 1 in siR-TIMP-3 group (B), while other two indicators including CD80 and iNOS were no significantly different in three groups at different days (A, C). The mRNA expression level of CD206, Arg-1 and Ym-1 increased at days 1, and 3 in siR-TIMP-3 group, among these, CD206 kept a relatively high level at day 7 (D, E, F). mRNA expression was relative to β-actin. ANOVA was used to process the data. Data are presented as mean + SEM, n = 6 for each time point. *P < 0.05, **P < 0.001.

4. Discussion

In this study, we identified TIMP-3 as a mediator of macrophage polarization and function in RPE/choroid tissues. It is the first time to demonstrate the absence of TIMP-3 could alter the macrophage differentiation, resulting in macrophages that are skewed toward a more pro-angiogenic polarization, with an increased expression of genes associated with M2 macrophages either in mouse and rat eyes with laser-induced photocoagulation or BMDM cells.

Clear evidences from animal models support dual roles for resident and invading macrophages/microglia in preventing and promoting neovascular AMD (Apte et al., 2006; Tsutsumi et al., 2003). The contradictory contributions of macrophages that have been observed in choroidal neovascularization might be explained by differential macrophage polarization with respect to M1 macrophages and M2 macrophages. Polarization is dynamic across time and involves the tissue microenvironment, one crucial aspect of monocyte differentiation into macrophages and their eventual polarization is the stereotypic alterations in cell surface marker expression, leading to increasing responsiveness to pro-inflammatory (M1) or pro-angiogenic (M2).

Although it has been shown that M2 macrophages promoted CNV development (He and Marneros, 2013; Wu et al., 2010), the underlying mechanisms remain elusive. It is known that TIMP-3 is critical in macrophage polarization in other tissues (Casagrande et al., 2012; Gill et al., 2013; Smookler et al., 2006). Casagrande V et al. have reported that TIMP-3 could affects atherosclerosis, likely through regulating

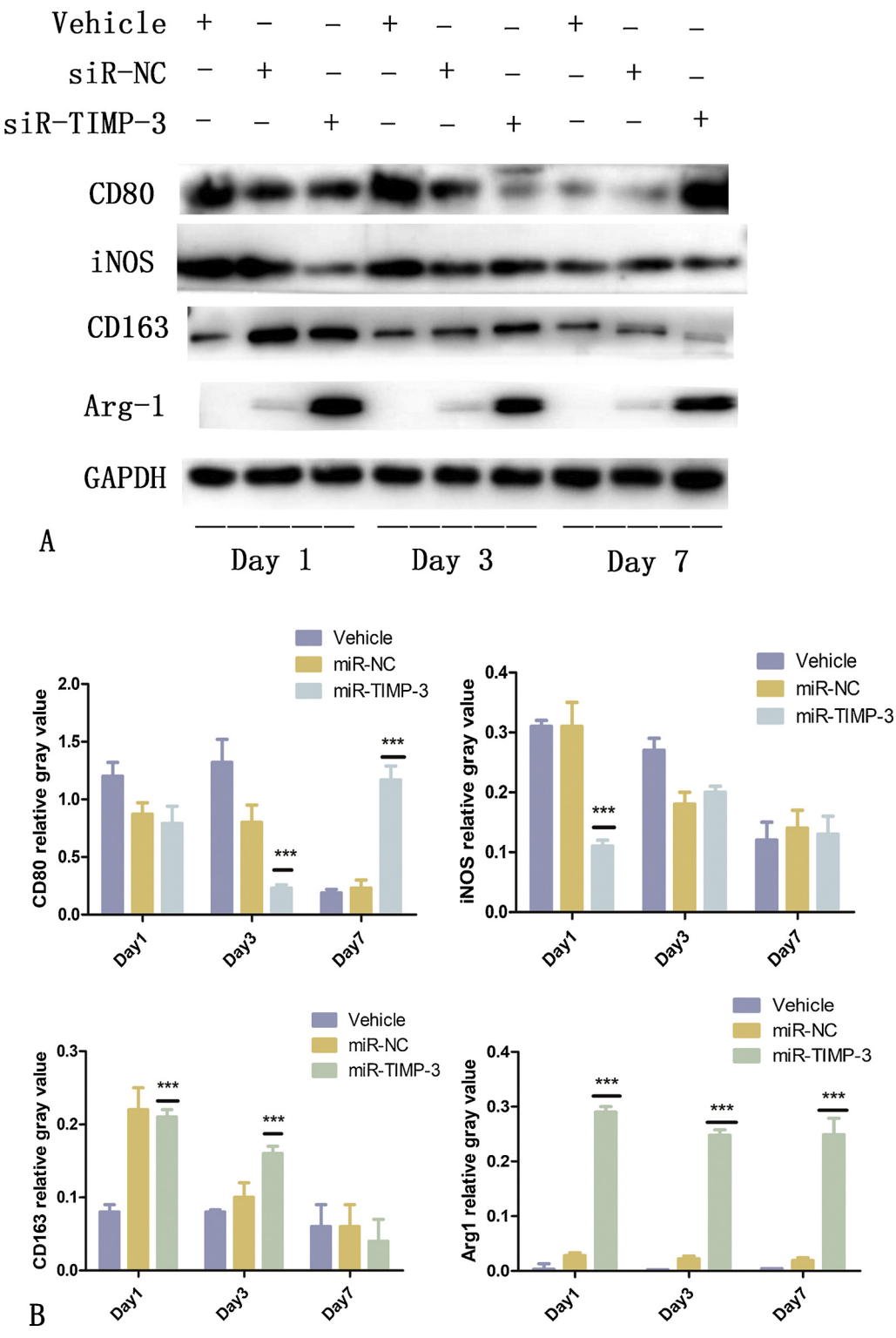

Fig. 5. Protein expression of CD80, iNOS, CD163 and Arg-1 in RPE/choroidal tissue after siRNA-TIMP-3 or negative control intravitreal injection at different time points in laser-induced CNV mice. The protein level of CD80 decreased at day 3, however, elevated at day 7 in siR-TIMP-3 group (A). iNOS protein expression declined at day 1 in siR-TIMP-3 group (B). The protein level of CD163 and Arg-1 significantly increased at days 1 and 3, and Arg-1 still kept a high protein level in day 7 (C, D). The protein expressions were relative to GAPDH. ANOVA was used to process the data. Data are presented as mean + SEM, n = 6 for each time point. *P < 0.05, **P < 0.001.

macrophage function (Apte et al., 2006). The overexpression of TIMP-3 in macrophages leads to smaller and more stable atherosclerotic plaques that contain fewer inflammatory cells (Casagrande et al., 2012), which indicates that increasing TIMP-3 expression in macrophages could protect against atherosclerotic plaque formation, and potentially promotes an anti-inflammatory phenotype in macrophages (M1). Besides, recent genomewide association scan analysis demonstrated TIMP-3 loci to be associated strongly with neovascular AMD (Lim et al., 2012; Yu et al., 2011). However, the role of TIMP-3 involved in macrophage polarization during CNV development is not resolved yet. Our data that macrophages were skewed toward pro-angiogenic polarization in absence of TIMP-3 microenvironment in retina, we assumed this phenomenon is involved in the changes of cytokines derived from the different macrophage polarization subtypes.

In mice, IL-10 produced by M2 phenotype was found to be a crucial factor driving abnormal angiogenesis, and inhibition of IL-10 decreased angiogenesis (Apte et al., 2006). What's more, a follow-up study found that both IL-10 levels and M2 polarization are increased in the retinal macrophage population of aged mice (Kelly et al., 2007). Hence, macrophage polarization might be a directing factor in AMD. In order

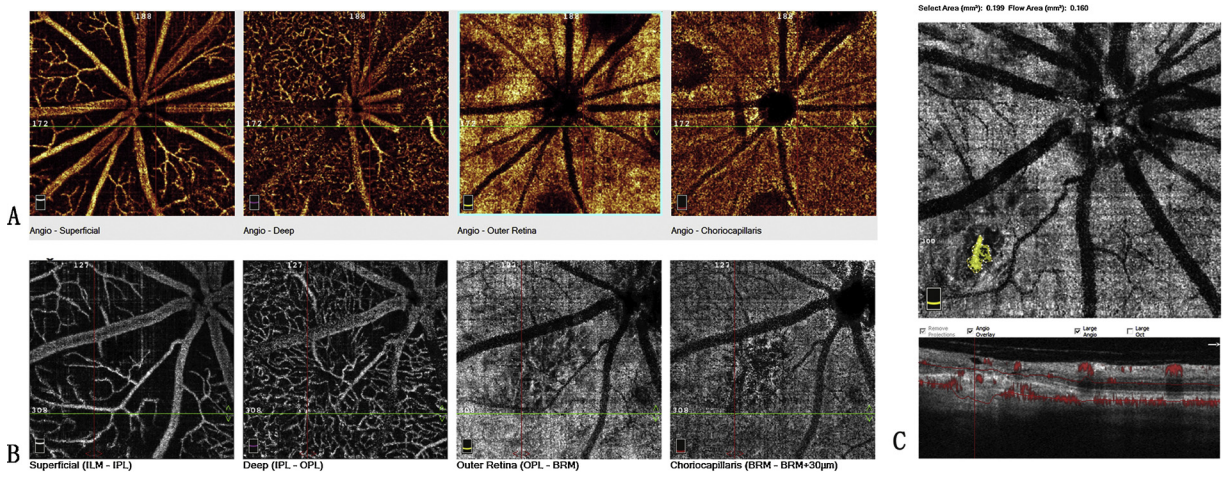

Fig. 6. OCT angiograms of a 6 × 6 mm^2 area visualizing blood flow in laser-induced CNV rats. (A) OCTA of the superficial (retinal ganglion cell and inner plexiform layers, large vessels radiating outwards from the optic nerve head to the periphery), deep (outer plexiform layer, dense plexus of capillaries) and outer (photoreceptors, no vessels and no blood flow detectable) retina and the choriocapillaris (high blood flow) in CNV animal model. Four laser burns were shown at 3, 6, 9 and 12 o'clock of the optic nerve, marked by white arrows. (B) OCTA visualizing the CNV net at outer retinal layer, marked with red arrow. (C) Quantitative features of CNV lesion (yellow area) including selected area and flow area are automatically calculated using AngioAnalytics software, corresponding OCT-b scan represented the hyperreflective CNV lesion broke the RPE layer (white arrow) (For interpretation of the references to colour in this figure legend, the reader is referred to the web version of this article).

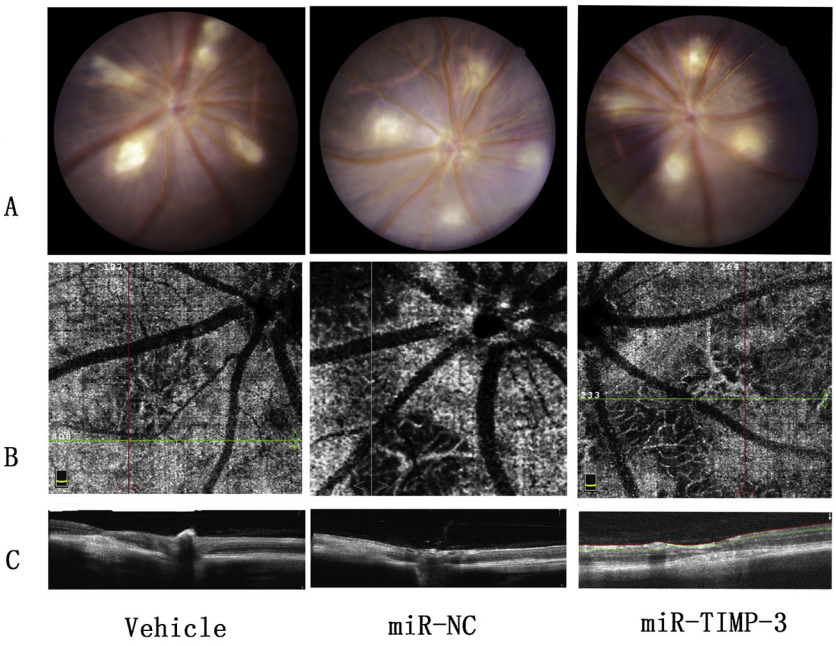

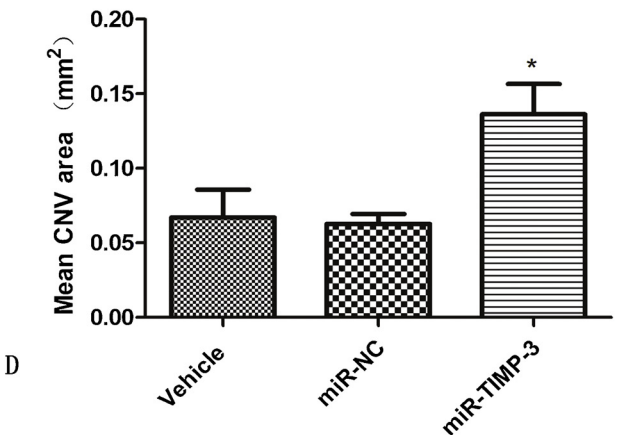

Fig. 7. Impact of TIMP-3 on CNV structure and flow area was detected by color fundus photography (Fig. 7A) and OCTA (Fig. 7B-C), CNV area in each eye was captured and automatically calculated by AngioAnalytics software. In our study, the mean CNV flow areas of vehicle, miR-NC and miR-TIMP-3 groups are 0.067 ± 0.038, 0.063 ± 0.013 and 0.136 ± 0.041 (P = 0.013), respectively, which demonstrated that intravitreal delivery of miR-TIMP-3 resulted in a significantly larger CNV flow area in comparison to control group at day 7 (Fig. 7D) (For interpretation of the references to colour in this figure legend, the reader is referred to the web version of this article).

to observe the microvascular growth and related pathological changes in mice retina, we used RTVue XR Avanti to obtain high-quality OCTA images of vascular plexus in the different retinal layers in the rat retina and choroid. It is possible to detect CNV quickly and to localize it in depth by simultaneous observation of the OCT scans using OCTA. With minimal variation of the segmentation and evaluating slabs obtained at the level of the hyperreflective material or subretinal fluid, it was possible to confirm a vascular component of this complex and to visualize the pathologic vessels in vivo for the first time in the laser-induced CNV rat model. What's more, it is also possible to contour the CNV and calculate the CNV area based on a binary image of the contoured area using AngioAnalytics, and these results measured by OCTA were consistent and repeatable (Alnawaiseh et al., 2016). In current study, we found the CNV area was smaller in the negative control group than siR-TIMP-3 group, which indicated the absence of TIMP-3 might accelerate the growth of CNV lesions in laser-induced rat model, in connection with macrophage polarization.

In current study, we suppressed the TIMP-3 expression using siRNA in BMDM and RPE/choroid tissues after laser-induced photocoagulation. The results have showed that the lack of TIMP-3 contributed to the M2 polarization, the M2 biomarkers including CD206, CD163, Arg-1 and Ym-1 expression increased in the siR-TIMP-3 group in both vitro and vivo, correspondingly. Hence, it is a critical finding that absence of TIMP-3 could result in M2 macrophages differentiation, we deduce that TIMP-3 could play a protective role in retina, and the decrease of TIMP-3 will lead to macrophage polarization toward M2 phenotypes with pro-angiogenic capacity in retina.

Collectively, we showed that TIMP-3 suppression leads to a more pro-angiogenic microenvironment, playing a key role in CNV formation by positively modulating M2 polarization. The role of TIMP-3 in the regulating inflammation and novel therapeutic target needs to be further studied.

Funding

This study was partly supported by National Natural Science foundation of China (31570789). The funder had no role in study design, data collection and analysis, decision to publish, or preparation of the manuscript.

Declaration of interest

The authors declare that they have no conflict of interest. The authors alone are responsible for the content and writing of the paper.

References

Alnawaiseh, M., Rosentreter, A., Hillmann, A., Alex, A.F., Niekamper, D., Heiduschka, P., Pap, T., Eter, N., 2016. OCT angiography in the mouse: A novel evaluation method for vascular pathologies of the mouse retina. Exp. Eye Res. 145, 417–423.

Apte, R.S., Barreiro, R.A., Duh, E., Volpert, O., Ferguson, T.A., 2004. Stimulation of neovascularization by the anti-angiogenic factor PEDF. Invest. Ophthalmol. Vis. Sci. 45, 4491–4497.

Apte, R.S., Richter, J., Herndon, J., Ferguson, T.A., 2006. Macrophages inhibit neovascularization in a murine model of age-related macular degeneration. PLoS Med. 3, e310.

Casagrande, V., Menghini, R., Menini, S., Marino, A., Marchetti, V., Cavalera, M., Fabrizi, M., Hribal, M.L., Pugliese, G., Gentileschi, P., Schillaci, O., Porzio, O., Lauro, D., Sbraccia, P., Lauro, R., Federici, M., 2012. Overexpression of tissue inhibitor of metalloproteinase 3 in macrophages reduces atherosclerosis in low-density lipoprotein receptor knockout mice. Arterioscler. Thromb. Vasc. Biol. 32, 74–81.

Espinosa-Heidmann, D.G., Suner, I.J., Hernandez, E.P., Monroy, D., Csaky, K.G., Cousins, S.W., 2003. Macrophage depletion diminishes lesion size and severity in experimental choroidal neovascularization. Invest. Ophthalmol. Vis. Sci. 44, 3586–3592.

Gill, S.E., Huizar, I., Bench, E.M., Sussman, S.W., Wang, Y., Khokha, R., Parks, W.C., 2010. Tissue inhibitor of metalloproteinases 3 regulates resolution of inflammation following acute lung injury. Am. J. Pathol. 176, 64–73.

Gill, S.E., Gharib, S.A., Bench, E.M., Sussman, S.W., Wang, R.T., Rims, C., Birkland, T.P., Wang, Y., Manicone, A.M., McGuire, J.K., Parks, W.C., 2013. Tissue inhibitor of metalloproteinases-3 moderates the proinflammatory status of macrophages. Am. J. Respir. Cell Mol. Biol. 49, 768–777.

Gordon, S., Martinez, F.O., 2010. Alternative activation of macrophages: mechanism and functions. Immunity 32, 593–604.

He, L., Marneros, A.G., 2013. Macrophages are essential for the early wound healing response and the formation of a fibrovascular scar. Am. J. Pathol. 182, 2407–2417.

Ishibazawa, A., Nagaoka, T., Takahashi, A., Omae, T., Tani, T., Sogawa, K., Yokota, H., Yoshida, A., 2015. Optical coherence tomography angiography in diabetic retinopathy: a prospective pilot study. Am. J. Ophthalmol. 160 (1).

Jager, R.D., Mieler, W.F., Miller, J.W., 2008. Age-related macular degeneration. N. Engl. J. Med. 358, 2606–2617.

Jia, Y., Morrison Jc Fau-Tokayer, J., Tokayer J Fau-Tan, O., Tan O Fau-Lombardi, L., Lombardi L Fau-Baumann, B., Baumann B Fau-Lu, C.D., Lu Cd Fau-Choi, W., Choi W Fau-Fujimoto, J.G., Fujimoto Jg Fau-Huang, D., Huang, D., 2012. Quantitative OCT angiography of optic nerve head blood flow. Biomed. Opt. Express 3.

Kelly, J., Ali Khan, A., Yin, J., Ferguson, T.A., Apte, R.S., 2007. Senescence regulates macrophage activation and angiogenic fate at sites of tissue injury in mice. J. Clin. Invest. 117, 3421–3426.

Lim, L.S., Mitchell, P., Seddon, J.M., Holz, F.G., Wong, T.Y., 2012. Age-related macular degeneration. Lancet (Lond., Engl.) 379, 1728–1738.

Penfold, P.L., Madigan Mc Fau - Gillies, M.C., Gillies Mc Fau - Provis, J.M., Provis, J.M., 2001. Immunological and aetiological aspects of macular degeneration. Prog. Retin. Eye Res. 20.

Quaranta-El Maftouhi, M., El Maftouhi, A., Eandi, C.M., 2015. Chronic central serous chorioretinopathy imaged by optical coherence tomographic angiography. Am. J. Ophthalmol. 160.

Sica, A., Erreni, M., Allavena, P., Porta, C., 2015. Macrophage polarization in pathology. Cell. Mol. Life Sci. 72, 4111–4126.

Smookler, D.S., Mohammed, F.F., Kassiri, Z., Duncan, G.S., Mak, T.W., Khokha, R., 2006. Tissue inhibitor of metalloproteinase 3 regulates TNF-dependent systemic inflammation. J. Immunol. (Baltimore, Md.: 1950) 176, 721–725.

Tanino, Y., Coombe, D.R., Gill, S.E., Kett, W.C., Kajikawa, O., Proudfoot, A.E., Wells, T.N., Parks, W.C., Wight, T.N., Martin, T.R., Frevert, C.W., 2010. Kinetics of chemokine-glycosaminoglycan interactions control neutrophil migration into the airspaces of the lungs. J. Immunol. (Baltimore, Md. : 1950) 184, 2677–2685.

Tsutsumi, C., Sonoda, K.H., Egashira, K., Qiao, H., Hisatomi, T., Nakao, S., Ishibashi, M., Charo, I.F., Sakamoto, T., Murata, T., Ishibashi, T., 2003. The critical role of ocular-infiltrating macrophages in the development of choroidal neovascularization. J. Leukoc. Biol. 74, 25–32.

Wu, W.K., Llewellyn, O.P., Bates, D.O., Nicholson, L.B., Dick, A.D., 2010. IL-10 regulation of macrophage VEGF production is dependent on macrophage polarisation and hypoxia. Immunobiology 215, 796–803.

Yu, Y., Bhangale, T.R., Fagerness, J., Ripke, S., Thorleifsson, G., Tan, P.L., Souied, E.H., Richardson, A.J., Merriam, J.E., Buitendijk, G.H., Reynolds, R., Raychaudhuri, S., Chin, K.A., Sobrin, L., Evangelou, E., Lee, P.H., Lee, A.Y., Leveziel, N., Zack, D.J., Campochiaro, B., Campochiaro, P., Smith, R.T., Barile, G.R., Guymer, R.H., Hogg, R., Chakravarthy, U., Robman, L.D., Gustafsson, O., Sigurdsson, H., Ortmann, W., Behrens, T.W., Stefansson, K., Uitterlinden, A.G., van Duijn, C.M., Vingerling, J.R., Klaver, C.C., Allikmets, R., Brantley Jr., M.A., Baird, P.N., Katsanis, N., Thorsteinsdottir, U., Ioannidis, J.P., Daly, M.J., Graham, R.R., Seddon, J.M., 2011. Common variants near FRK/COL10A1 and VEGFA are associated with advanced age-related macular degeneration. Hum. Mol. Genet. 20, 3699–3709.

Zhao, H., Roychoudhury, J., Doggett, T.A., Apte, R.S., Ferguson, T.A., 2013. Age-dependent changes in FasL (CD95L) modulate macrophage function in a model of age-related macular degeneration. Invest. Ophthalmol. Vis. Sci. 54, 5321–5331.